

## Electronic Supplementary Information

### Panchromatic Small Molecules for UV-Vis-NIR Photodetectors with High Detectivity

Ji Qi,<sup>a,b</sup> Liang Ni,<sup>a</sup> Dezhi Yang,<sup>a</sup> Xiaokang Zhou,<sup>a,b</sup> Wenqiang Qiao,<sup>\*a,d</sup> Mao Li,<sup>a</sup> Dongge Ma<sup>a</sup> and Zhi Yuan Wang<sup>\*a,c</sup>

<sup>a</sup> State Key Laboratory of Polymer Physics and Chemistry, Changchun Institute of Applied Chemistry, Chinese Academy of Sciences, Changchun, China 130022

<sup>b</sup> University of Chinese Academy of Sciences, Beijing, China 100049

<sup>c</sup> Department of Chemistry, Carleton University, 1125 Colonel By Drive, Ottawa, Ontario, Canada K1S 5B6

<sup>d</sup> School of Materials Science and Engineering, Harbin Institute of Technology, Harbin, China 150001

\*To whom correspondence should be addressed. E-mail: wayne\_wang@carleton.ca; wqqiao@ciac.ac.cn

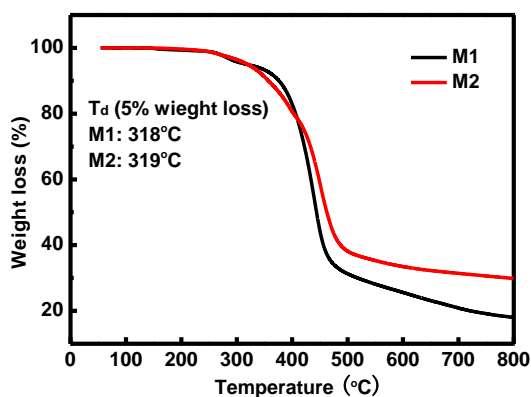
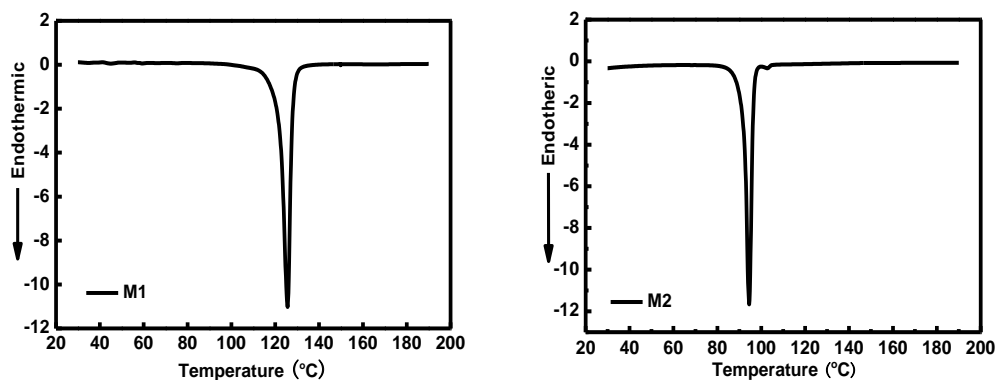


Fig. S1 TGA traces of M1 and M2 under nitrogen atmosphere.



**Fig. S2** DSC of M1 and M2 under nitrogen atmosphere.

**Table S1. Optical and Electrochemical Data of M1 and M2**

Compound	Abs. <sup>a</sup> /nm	Abs. <sup>b</sup> /nm	$\epsilon^c/\text{cm}^{-1}$	HOMO <sup>d</sup>	LUMO <sup>d</sup>	E <sub>g</sub> /eV
M1	713	782	49514	-4.80/0.32	-3.65/-0.83	1.15
M2	718	770	35196	-4.77/0.29	-3.65/-0.83	1.12

<sup>a</sup> Solution: measured in DCM with a concentration of  $1 \times 10^{-5}$  M. <sup>b</sup> Film: spin-coated on quartz plate. <sup>c</sup> Absorption coefficient of the low-energy absorption peak of the film. <sup>d</sup> Calculated from the formula, E (HOMO) =  $-(E_{\text{ox}} + 4.48)$  (eV), E (LUMO) =  $-(E_{\text{red}} + 4.48)$  (eV).

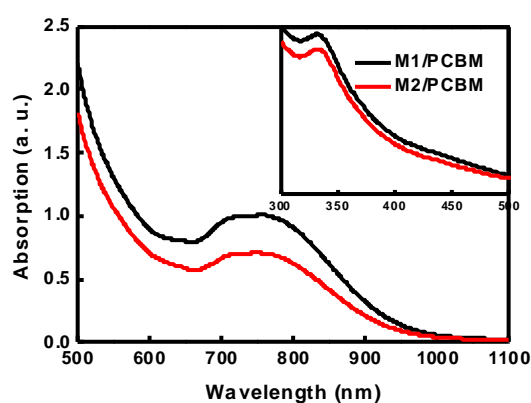


**Fig. S3** Absorption spectra of the films of M1/M2 and PCBM (1:3 by weight) spin-coated on quartz plate.

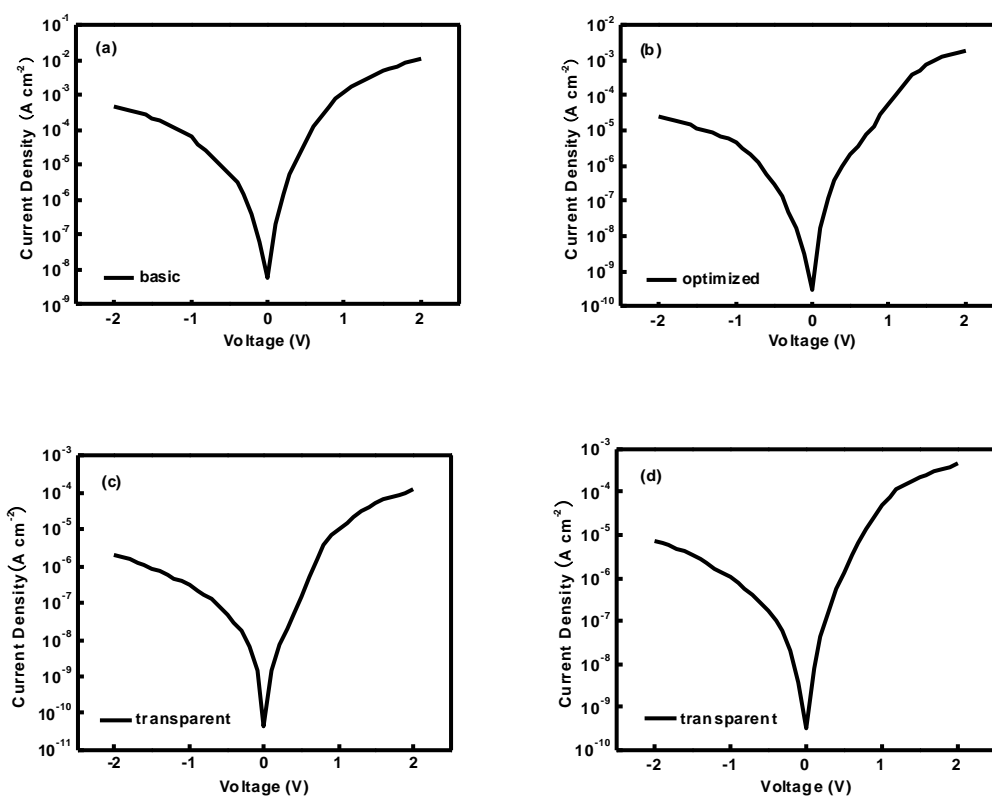


**Fig. S4** Current density-voltage ( $J$ - $V$ ) characteristics of the devices in the dark. (a) device b; (b) device d; (c) device e; (d) device f.

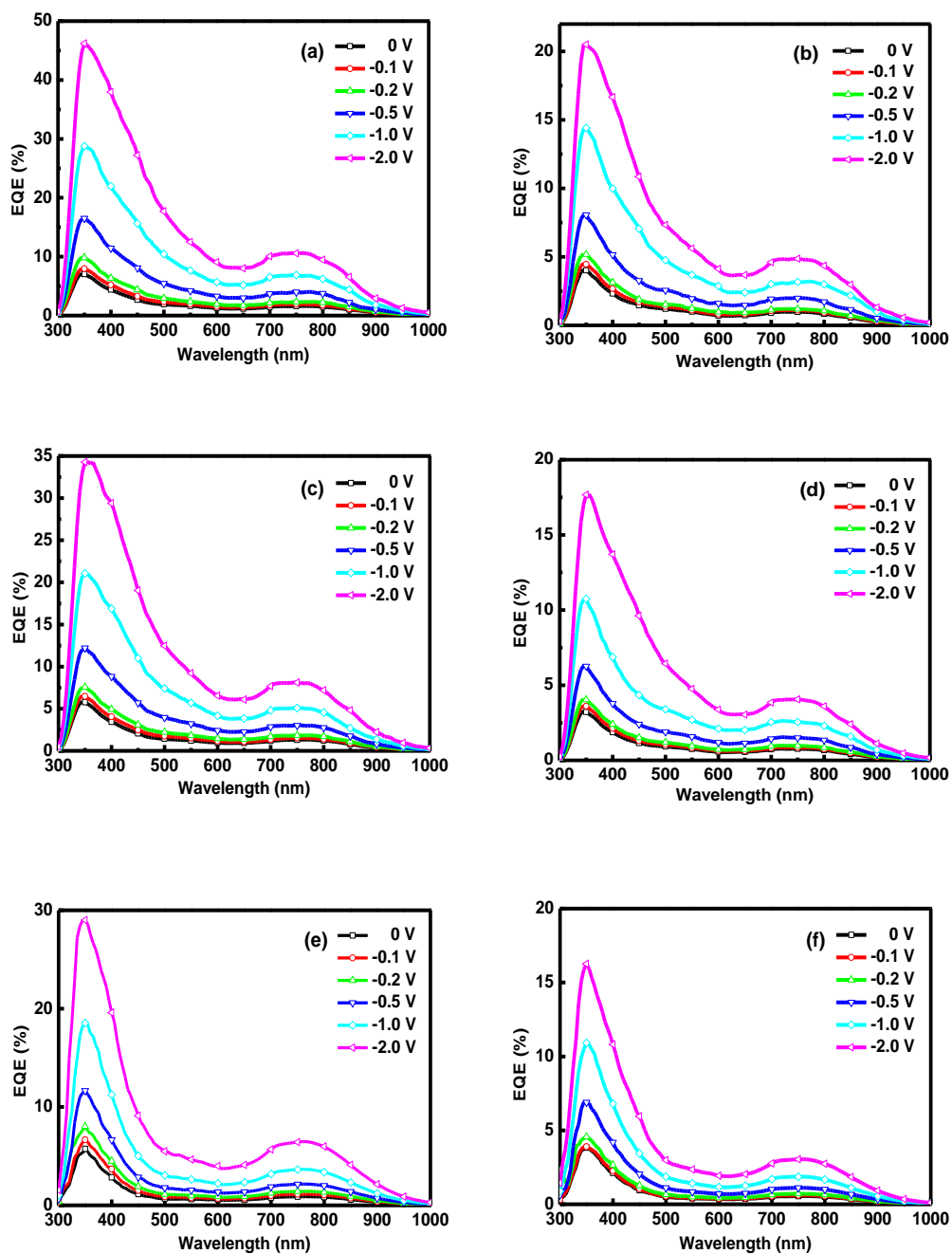
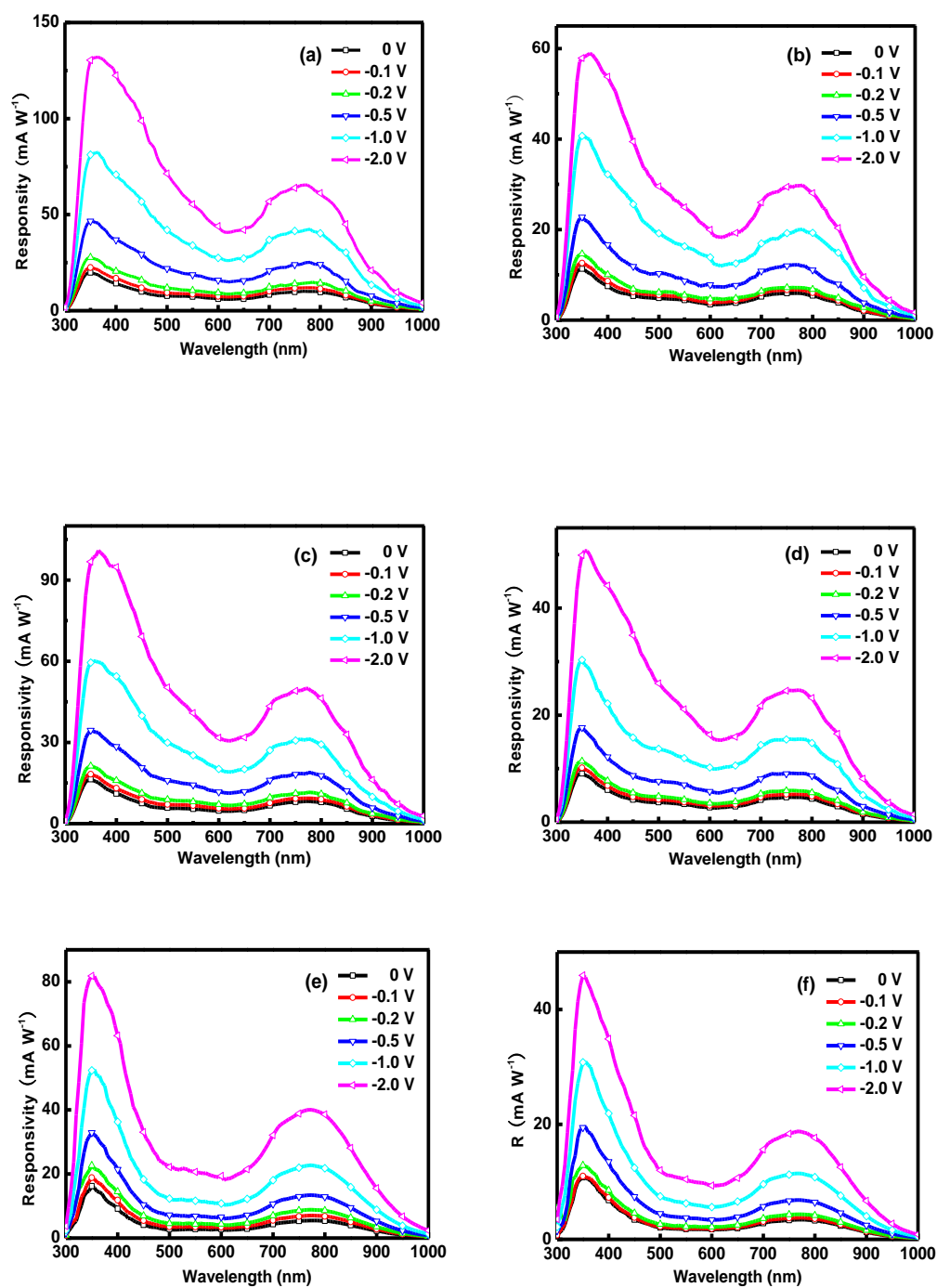
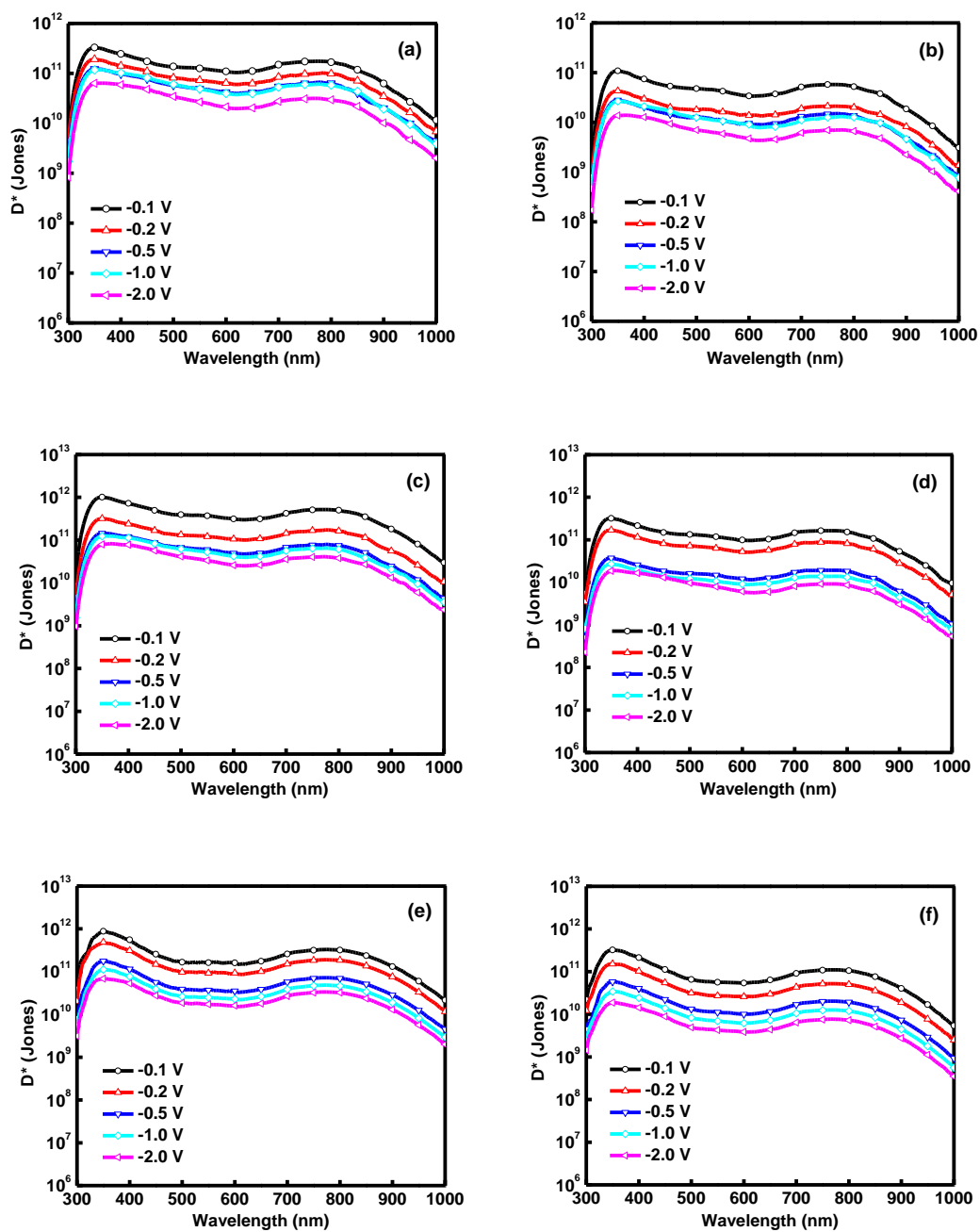


Fig. S5 EQE of device a to device f at different biases.



**Fig. S6** Responsivity ( $R$ ) of device a to device f at different biases.



**Fig. S7** Specific detectivity ( $D^*$ ) of device a to device f at different biases.

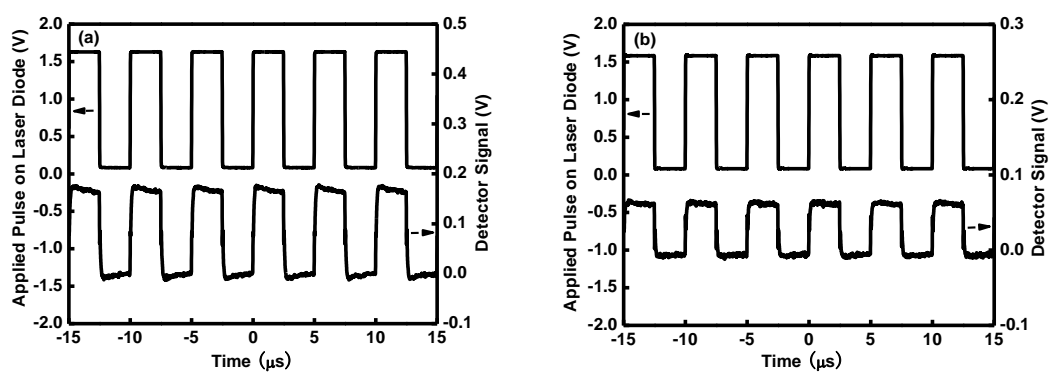


**Fig. S8** Transient response of device c (a) and d (b) at a biased voltage of -0.1 V under 0.1 MHz modulation with 550 nm monochromatic illumination.

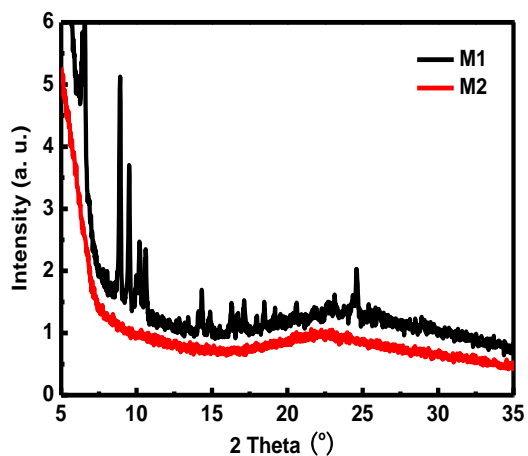


**Fig. S9** Wide angle X-ray diffraction (WAXRD) diagrams of M1 and M2 drop-cast on glass substrate.

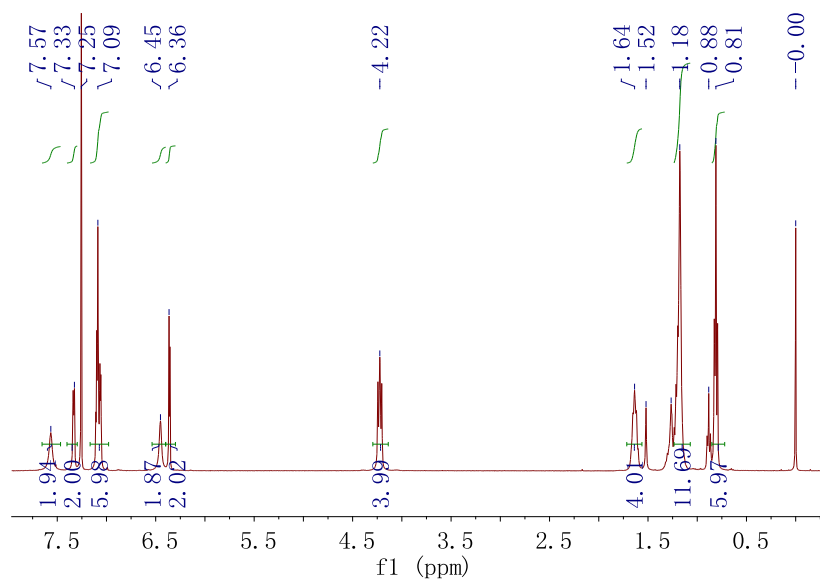


**Fig. S10**  $^1\text{H}$  NMR (400 MHz,  $\text{CDCl}_3$ , 298 K) of **M1**.

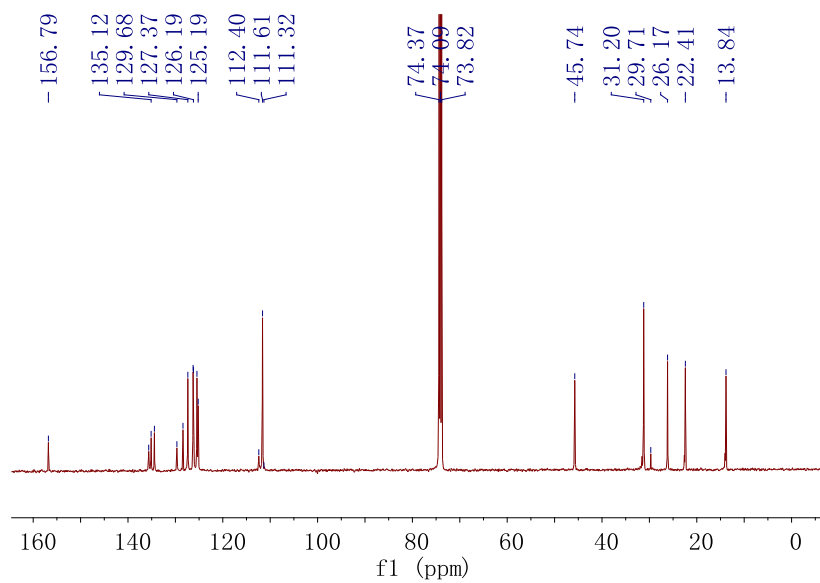


**Fig. S11**  $^{13}\text{C}$  NMR (100 MHz,  $\text{C}_2\text{D}_2\text{Cl}_4$ , 373 K) of **M1**.



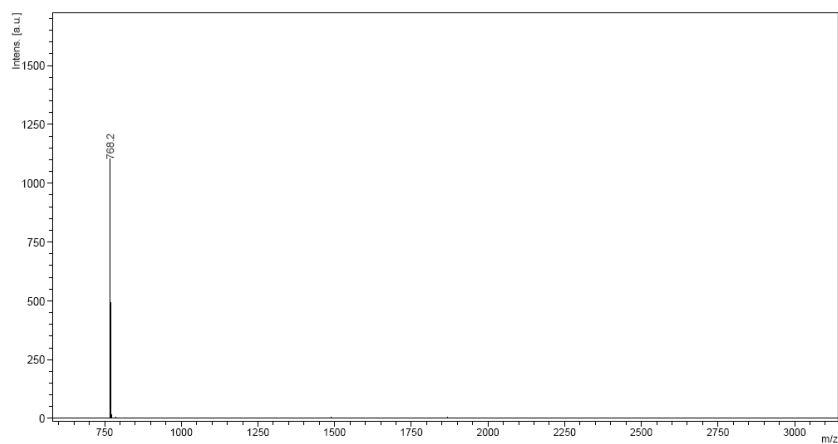


**Fig. S12** MALDI-TOF MS of **M1**.

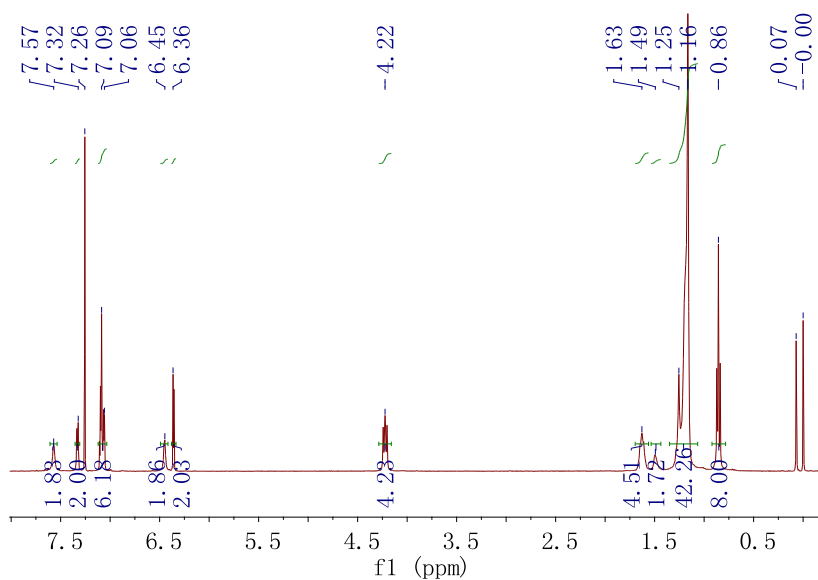


**Fig. S13** <sup>1</sup>H NMR (400 MHz, CDCl<sub>3</sub>, 298 K) of **M2**.

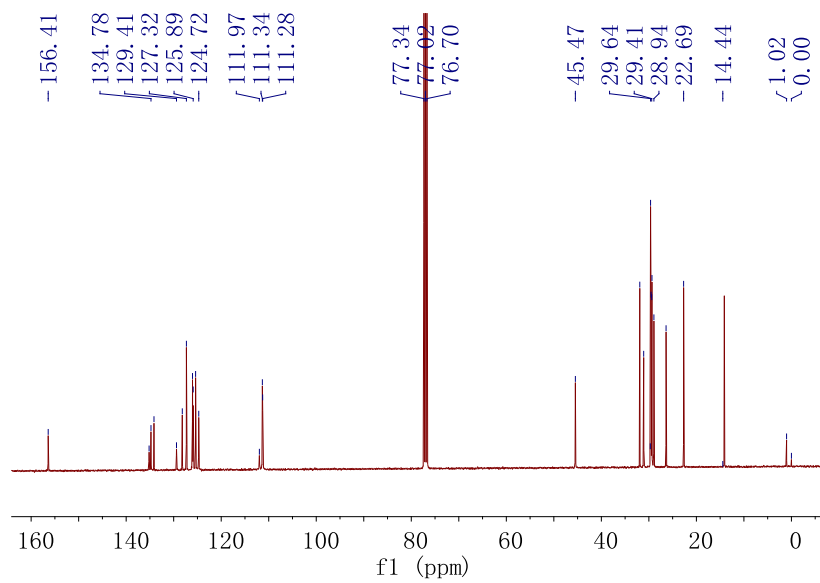


**Fig. S14**  $^{13}\text{C}$  NMR (100 MHz,  $\text{CDCl}_3$ , 298 K) of **M2**.

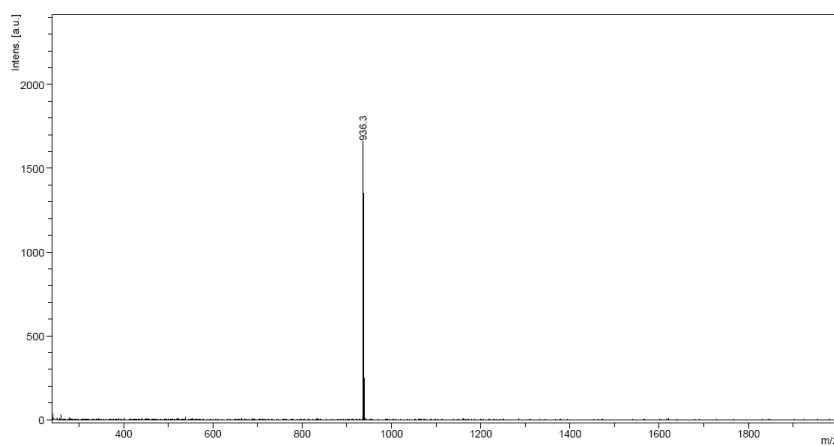


**Fig. S15** MALDI-TOF MS of **M2**.